

# Population Genomic Analysis Reveals Contrasting Demographic Changes of Two Closely Related Dolphin Species in the Last Glacial

Nagarjun Vijay,<sup>†,1</sup> Chungoo Park,<sup>†,2</sup> Jooseong Oh,<sup>2</sup> Soyeong Jin,<sup>3</sup> Elizabeth Kern,<sup>3</sup> Hyun Woo Kim,<sup>4</sup> Jianzhi Zhang,<sup>\*,1</sup> and Joong-Ki Park<sup>\*,3</sup>

<sup>1</sup>Department of Ecology and Evolutionary Biology, University of Michigan, Ann Arbor, MI

<sup>2</sup>School of Biological Sciences and Technology, Chonnam National University, Gwangju, Republic of Korea

<sup>3</sup>Division of EcoScience, Ewha Womans University, Seoul, Republic of Korea

<sup>4</sup>Cetacean Research Institute, National Institute of Fisheries Science, Ulsan, Republic of Korea

<sup>†</sup>These authors are co-first authors.

\*Corresponding authors: E-mails: jianzhi@umich.edu; jkpark@ewha.ac.kr.

Associate editor: Yoko Satta

## Abstract

Population genomic data can be used to infer historical effective population sizes ( $N_e$ ), which help study the impact of past climate changes on biodiversity. Previous genome sequencing of one individual of the common bottlenose dolphin *Tursiops truncatus* revealed an unusual, sharp rise in  $N_e$  during the last glacial, raising questions about the reliability, generality, underlying cause, and biological implication of this finding. Here we first verify this result by additional sampling of *T. truncatus*. We then sequence and analyze the genomes of its close relative, the Indo-Pacific bottlenose dolphin *T. aduncus*. The two species exhibit contrasting demographic changes in the last glacial, likely through actual changes in population size and/or alterations in the level of gene flow among populations. Our findings suggest that even closely related species can have drastically different responses to climatic changes, making predicting the fate of individual species in the ongoing global warming a serious challenge.

**Key words:** climate change, genome sequencing, population structure, *Tursiops aduncus*, *Tursiops truncatus*.

Understanding the impact of a rapidly changing climate on biodiversity represents an urgent challenge due to the ongoing global warming (Thuiller 2007). Although the causes of past and present climatic changes may be different, the consequences of past climatic changes on biodiversity can provide useful insights. Hence, a promising approach is to use population genomic data to infer historical effective population sizes ( $N_e$ ) and study how  $N_e$  has responded to past climatic change events such as Pleistocene glacial cycles. This approach has frequently revealed a reduction in  $N_e$  during the last glacial (110–12 kya) for temperate species, including marine cetaceans (Moura et al. 2014; Yim et al. 2014). Surprisingly, however, the genomic analysis of one individual of the common bottlenose dolphin *Tursiops truncatus* suggested a steep rise in  $N_e$  in the last glacial (Yim et al. 2014), raising questions about the reliability, generality, underlying cause, and biological implication of this finding. In the present study, we first verify the previous finding by additional sampling of *T. truncatus*. We then sequence and analyze the genomes of its closest congener, the Indo-Pacific bottlenose dolphin *T. aduncus*, for comparison. We report contrasting demographic changes of these two species in the last glacial, explore potential causes, and discuss implications.

Bottlenose dolphins (genus *Tursiops*) include at least two taxonomically accepted, widespread species: *T. truncatus* and

*T. aduncus*. According to a recent estimate based on both mitochondrial and nuclear markers, these two species diverged from each other  $\sim 0.7$  Ma (Gray et al. 2018). The use of more markers and widespread sampling makes this a more reliable estimate than the previously reported divergence time of  $\sim 2.5$  Ma (Vilstrup et al. 2011). The two dolphin species occupy distinct but overlapping habitats and regions (Hale et al. 2000): *T. truncatus* is distributed in the coastal, near-shore, and off-shore zones of most oceans worldwide, with the exception of polar areas, whereas *T. aduncus* is discontinuously distributed along the coastal areas of warm temperate and tropical Indian and Indo-Pacific oceans, from east Africa to the northwestern Pacific (fig. 1).

We used the Pairwise Sequentially Markovian Coalescent (PSMC) method (see Materials and Methods) to, respectively, infer the temporal changes in  $N_e$  from publically available genome sequences of four *T. truncatus* individuals, including the one previously analyzed (Yim et al. 2014; supplementary table S1, Supplementary Material online). For all four genomes,  $N_e$  rose sharply starting around the beginning of the last glacial, peaked when the atmosphere temperature reached the minimum, and then dropped as the temperature rebounded (fig. 2). Bootstrap analysis confirms the statistical robustness of these trends (supplementary fig. S1A, Supplementary Material online).

© The Author(s) 2018. Published by Oxford University Press on behalf of the Society for Molecular Biology and Evolution.

This is an Open Access article distributed under the terms of the Creative Commons Attribution Non-Commercial License (<http://creativecommons.org/licenses/by-nc/4.0/>), which permits non-commercial re-use, distribution, and reproduction in any medium, provided the original work is properly cited. For commercial re-use, please contact [journals.permissions@oup.com](mailto:journals.permissions@oup.com)

Open Access

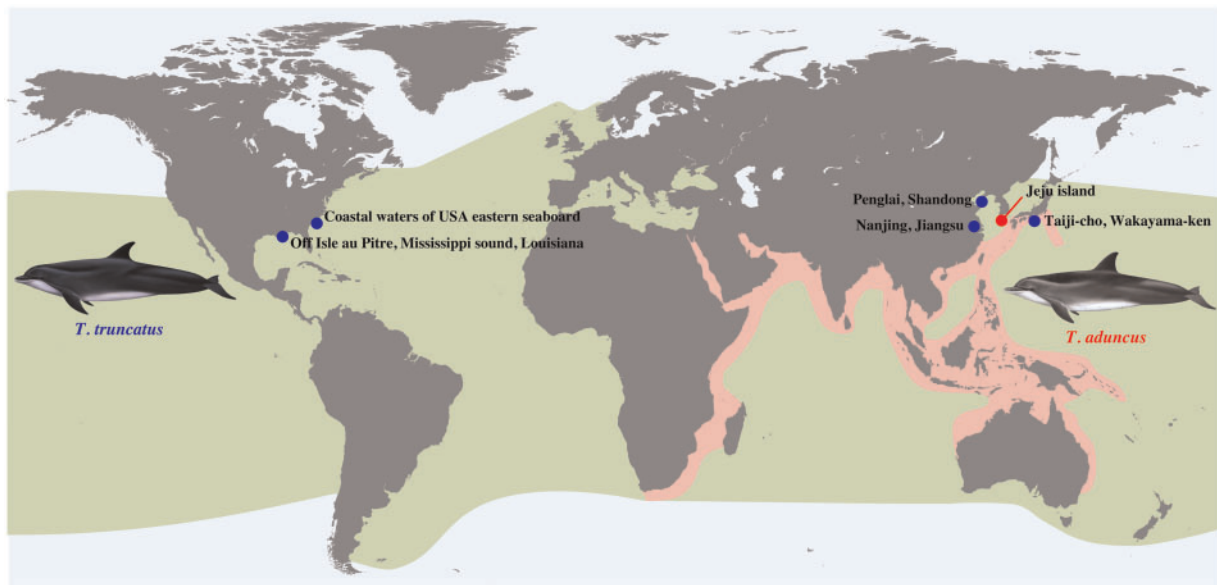


**FIG. 1.** Map showing the geographic distributions of the common bottlenose dolphin *Tursiops truncatus* (green) and Indo-Pacific bottlenose dolphin *T. aduncus* (pink). The map is redrawn from the IUCN red list resource.shp file. See Materials and Methods for details.

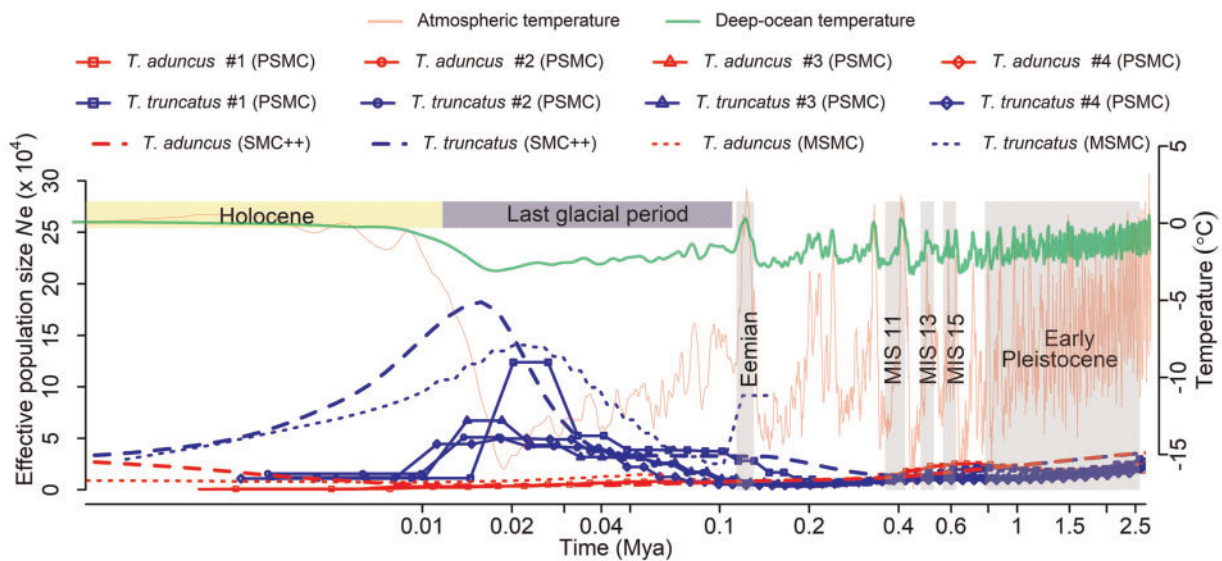


**FIG. 2.** Contrasting demographic changes of the two bottlenose dolphin species in the last glacial, inferred from genome sequences using PSMC, MSMC, and SMC++. MIS, Marine Isotope Stage. All dolphins whose genomes are analyzed here are from Northwest Pacific. See [supplementary table S1, Supplementary Material](#) online for detailed information of individual dolphin genomes.

To probe whether this unusual demographic pattern is specific to *T. truncatus*, we generated a high-quality de novo genome assembly for *T. aduncus*, using 180× coverage of Illumina sequencing of an individual sampled from Korea, followed by sequencing of three additional individuals at lower coverages (22–32×; [supplementary tables S1 and S2, Supplementary Material](#) online; see Materials and Methods). Population genomic analyses were conducted using four *T. truncatus* and four *T. aduncus* individuals. Nucleotide diversity ( $\pi$ ) is greater for *T. truncatus* (0.0015) than *T. aduncus* (0.00095), as expected from the wider geographic distribution of the former than the latter. The two

species exhibit high levels of genome-wide differentiation (mean  $F_{st} = 0.61$ ), consistent with their different geographic distributions and classification as distinct species (with the caveat that this conclusion is based on Northwest Pacific *T. truncatus*; see below). The PSMC analysis of each *T. aduncus* individual shows a decline in  $N_e$  during the last glacial ([fig. 2](#) and [supplementary fig. S1A, Supplementary Material](#) online). This prolonged decline started  $>0.5$  Ma, and no rebound since then is apparent ([fig. 2](#)). The PSMC-inferred, contrasting patterns of  $N_e$  between the two dolphin species are robust to different generation times and mutation rates assumed ([supplementary fig. S1B, Supplementary Material](#) online) and are

confirmed by MSMC and SMC++ (fig. 2), which are improved methods that can simultaneously analyze multiple genome sequences (see Materials and Methods). The population size trajectories that have not been scaled by mutation rate and generation time also show a clear distinction between the two species (supplementary fig. S1C, Supplementary Material online).

All individuals of *T. truncatus* and *T. aduncus* analyzed above were sampled from Northwest Pacific (off the coasts of China, Korea, and Japan) and are thus more or less comparable. The public domain also houses the genome sequences from two individuals of *T. truncatus* from the Northwest Atlantic, sampled off Isle au Pitre in the Mississippi Sound, Louisiana and the coastal waters of the US eastern seaboard, respectively (supplementary table S1, Supplementary Material online). As expected, principal component analysis shows that all *T. truncatus* individuals are genetically distinct from *T. aduncus* (supplementary fig. S2, Supplementary Material online). The four *T. aduncus* individuals are genetically highly similar (supplementary fig. S2, Supplementary Material online). Within *T. truncatus*, however, the two Northwest Atlantic individuals are genetically quite distinct from each other and from the four Northwest Pacific individuals (supplementary fig. S2, Supplementary Material online), suggesting population differentiation of *T. truncatus*. Analyses of the 3rd and 4th principal components show population structure even within Northwest Pacific *T. truncatus* (supplementary fig. S2, Supplementary Material online). Strikingly, the Louisiana (Northwest Atlantic) individual has a temporal trend of  $N_e$  highly similar to those of *T. aduncus* individuals, with a decline in  $N_e$  in the last glacial (supplementary fig. S3, Supplementary Material online). The genome sequence coverage of the US eastern seaboard (Northwest Atlantic) individual ( $0.7\times$ ) is too low to allow a reliable PSMC analysis.

Because the tremendous temporal changes of  $N_e$  for (Northwest Pacific) *T. truncatus* coincided well with the drastic atmosphere and deep-ocean temperature changes of the last glacial (fig. 2), the demographic changes were potentially caused directly or indirectly by the climatic changes. Global cooling could directly affect dolphin habitats and distributions because of lowered sea levels and reduced ocean temperatures (Learmonth et al. 2006). Although these effects could explain the  $N_e$  decline for the coastal species *T. aduncus*, they cannot easily explain the  $N_e$  increase for the broadly distributed *T. truncatus*. Global climate change could have also affected dolphins through food availability due to alterations in currents, upwelling, and productivity, and through the altered ecology of pathogens, competitors, and predators (Hoegh-Guldberg and Bruno 2010). It is notable that the  $N_e$ 's of some dolphin predators declined during the last glacial, which could lead to a surge in dolphin  $N_e$ . For instance, dolphins are preyed upon by some large sharks, most of which are restricted to the warmer tropical climates. In general, sharks in warm zones show genetic signatures of reduced  $N_e$  in the last glacial (O'Brien et al. 2013). Furthermore, killer whales show a decline in  $N_e$  at the same period (Moura et al. 2014). Killer whales are more abundant in *T. truncatus*' habitat

than *T. aduncus*' habitat at the present (Forney and Wade 2006). If these species had similar distributions during the last glacial, *T. truncatus* may have benefited more than *T. aduncus* from killer whale's decline in the last glacial. Although dolphins are a relatively minor part of the diet of killer whales today, it is possible that climate changes indirectly caused the contrasting trends of  $N_e$  between *T. truncatus* and *T. aduncus* by differentially impacting their predators.

Temporal changes in  $N_e$  can also be caused by alterations in population structure or gene flow between populations (Mazet et al. 2016). Marine mammals with their complex patterns of ancestry can especially be influenced by such processes (Foote and Morin 2016). To examine this possibility in the dolphins, we conducted a PSMC analysis of pseudo-diploids artificially constructed from genomes of two different individuals (see Materials and Methods). Pseudo-diploids made from two different *T. aduncus* individuals and actual *T. aduncus* individuals show almost identical temporal trends of  $N_e$  (fig. 3), confirming a lack of population structure in this species. For (Northwest Pacific) *T. truncatus*, however, all pseudo-diploids show a much greater  $N_e$  from 0.1 to 0.2 Ma to the present (fig. 3), which is a sign of population structure, echoing a previous genetic-marker-based study that showed population structure of *T. truncatus* in Northeast Atlantic despite no obvious barrier to gene flow (Louis et al. 2014) and a report that coastal *T. truncatus* exhibits strong population structure even in geographically close populations (Martien et al. 2012). Our pseudo-diploid result, coupled with the hump in  $N_e$  from the real *T. truncatus* individuals during the last glacial (fig. 2), suggests a reduction in gene flow among *T. truncatus* populations in this period (Mazet et al. 2016), which was potentially caused directly or indirectly by the global cooling.

In line with the population structure inferred from the principal component analysis (supplementary fig. S2, Supplementary Material online), PSMC analysis shows an earlier substantial rise in  $N_e$  for pseudo-diploids constructed between Louisiana and Northwest Pacific *T. truncatus* individuals than for pseudo-diploids between Northwest Pacific individuals (supplementary fig. S4, Supplementary Material online). SMC++ split analysis using the joint frequency spectrum confirms the PSMC results of pseudo-diploids by showing much earlier split times between *T. truncatus* individuals than between *T. aduncus* individuals (supplementary fig. S5, Supplementary Material online). A previous study around the main Hawaiian Islands suggested hybridization between *T. truncatus* and *T. aduncus* (Martien et al. 2012). We thus also used PSMC to analyze pseudo-diploids constructed between *T. truncatus* and *T. aduncus* individuals. We found that the split times between the two species ( $\geq 0.3$  Ma; supplementary fig. S6, Supplementary Material online) were much earlier than the split times found within *T. truncatus* (supplementary fig. S4, Supplementary Material online). The  $N_e$ 's of interspecific pseudo-diploids rose substantially in a step-wise manner, suggesting postdivergence gene flow (Song et al. 2014, 2017). The timing of the initial increase in  $N_e$  is thought to approximate the split time,

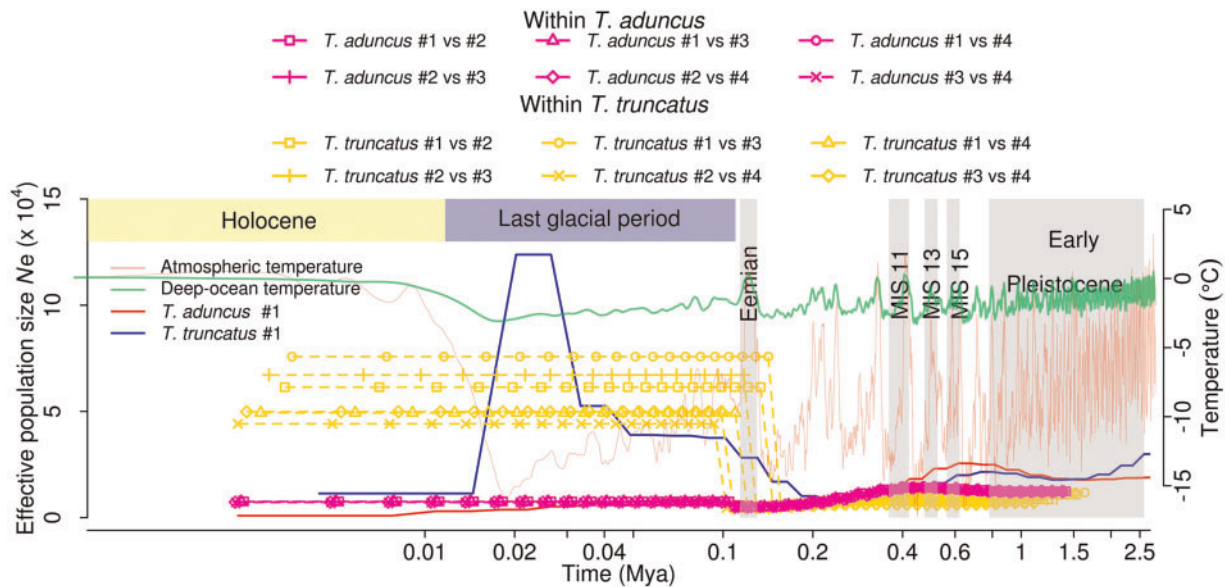


**Fig. 3.** Pseudo-diploid analysis using PSMC suggests population structure in (Northwest Pacific) *T. truncatus* (yellow lines) but not *T. aduncus* (violet lines).

and the presence of a series of split times instead of a single abrupt split time for all sampled individuals suggests a stepwise process of splitting up between the two species and/or ancient introgressions. However, more widespread sampling of individuals especially from populations that have been the focus of long-term observational studies will be required to acquire a better understanding of population structure. A recent study by Gray et al. (2018) supports this stepwise process of splitting of *Tursiops* lineages between 1 and 0.7 Ma.

In summary, our population genomic analysis revealed contrasting temporal trends of  $N_e$  in the last glacial between two closely related dolphin species and potentially even between populations within a single species, likely due to complex and often idiosyncratic ecological interactions that vary between species or populations, including for example changes in predator population sizes and migration rates among populations. Such variations make it possible for closely related species and populations to respond drastically differently to the same climate event. The pattern reported here is unlikely to be unique to bottlenose dolphins, because similar contrasts were previously inferred for sea snails (Albaina et al. 2012) and beltfish (He et al. 2015) on the basis of much smaller data and in minke whales on the basis of genomic data of fewer samples (Kishida 2017). Hence, predicting the impact of climate change on a particular species or population may be difficult without a much greater understanding of the specific ecological and biological factors involved.

## Materials and Methods

### Spatial Distribution Data

Spatial distribution data for >50 thousand species were collated by the International Union for Conservation of Nature (IUCN) as a resource to accompany the Red List of Threatened Species. This data set is available for

download as .shp files at <http://www.iucnredlist.org/technical-documents/spatial-data>; last accessed May 25, 2018. We downloaded the data corresponding to Marine Mammals Group on December 29, 2016. Because this shapefile contains data for many marine mammals, we subsetted the data to the spatial distribution of *T. truncatus* and *T. aduncus* using the R package `mapproj`. The spatial locations of the sampling points were then added to the figure. Dolphin images were added to the spatial distribution map.

### Dolphin Samples

*T. aduncus* and *T. truncatus* were considered monospecific until the recognition of two species on the basis of genetic evidence and morphology (osteology and external morphology including beak morphology, dorsal fin shape, and the presence/absence of ventral spotting in adults; Wang et al. 1999, 2000a, 2000b). More recently, molecular evidence suggests that *T. aduncus*, long-beaked common dolphin *Delphinus capensis*, and striped dolphin *Stenella coeruleoalba* form a monophyletic clade that is sister to *T. truncatus* (Leduc et al. 1999; Vilstrup et al. 2011; Moura et al. 2013).

Tissue samples of four individuals of *T. aduncus* were obtained from stranded dead individuals on the coast of Jeju Island, Korea. Sex was recorded in the field, and confirmed by subsequent genetic analysis. We generated whole-genome sequencing data at  $\sim 180\times$  coverage (based on an estimated 2.29 Gb genome size; supplementary table S1, Supplementary Material online) for one individual and resequencing data of  $22\text{--}32\times$  coverage for the remaining three individuals (supplementary table S1, Supplementary Material online). These data were supplemented with publicly available sequences of six individuals of *T. truncatus* (four from Northwest Pacific and two from Northwest Atlantic) downloaded from the Short Read Archive (SRA). Sampling of *T. truncatus* from the Northwest Pacific is widespread, spanning over 1,000 km.

Details of the coverage, sex, and SRA accession numbers of all samples are provided in [supplementary table S1, Supplementary Material](#) online.

### Genomic DNA Library Construction, Sequencing, and Assembly

Genomic DNA was extracted from muscle tissues using the DNeasy Blood & Tissue kit (Qiagen, Germany). Extracted DNA was quantified by the Quant-iT BR assay kit (Invitrogen). For the reference genome of *T. aduncus*, we constructed short-insert (350 and 550 bp with  $2 \times 251$  bp reads) and long-insert (5 and 10 kb with  $2 \times 101$  bp reads) libraries using the standard protocol provided by Illumina (San Diego, USA). Three additional *T. aduncus* individuals were subjected to  $2 \times 150$  bp paired-end sequencing of a 350 bp insert library. The raw reads were preprocessed using Trimmomatic v0.33 (Bolger et al. 2014) and Trim Galore (Martin 2011), in which reads containing adapter sequences, poly-N sequences, or low-quality bases (below a mean Phred score of 20) were removed. For the reference genome assembly of *T. aduncus*, we used all preprocessed reads from four (350 bp, 550 bp, 5 kb, and 10 kb) libraries and employed ALLPATHS-LG v52488 (Gnerre et al. 2011). Next, gaps (any nucleotide represented by “N” in scaffolds) were closed using GapCloser, a module of SOAPdenovo2 (Luo et al. 2012). For further analyses, any scaffold with  $>0.04\%$  hits belonging to bacterial genomes from NCBI (release of Nov. 2016), downloaded from the RefSeq microbial genomes ftp site (Tatusova et al. 2014), was removed. A draft genome was assembled for *T. aduncus* using both paired-end and mate-pair libraries. The final assembled genome is 2.5 Gb in total length, close to the estimate by K-mer analysis (2.29 Gb), and was composed of 16,188 scaffolds ( $\geq 1$  kb in their length) with an N50 value of 1,254 kb ([supplementary table S2, Supplementary Material](#) online). The assembly was found to be of good quality; 95.2% of the core eukaryotic genes (based on 248 core essential genes) from CEGMA v2.5 (Parra et al. 2007), 89.7% of the core vertebrate genes (based on 233 one-to-one orthologs in vertebrate genomes) previously identified (Hara et al. 2015), and 92.1% of the metazoan single-copy orthologs (based on 843 genes) from BUSCO v1.22 (Simão et al. 2015) could be identified in the genome assembly. Among these 92.1% of genes identified, 82.3%, 5.0%, and 4.7% are complete single-copy, complete duplicate, and partial genes, respectively.

### Read Mapping and Variant Calling

The genome assembly and annotation of *T. truncatus* release-87 were downloaded from Ensembl. The sequencing reads from each dolphin species were mapped to the genome assembly using the Burrows–Wheeler aligner BWA-MEM (Li 2013), with default settings. PCR duplicate reads were collapsed using the rmdup option in SAMtools (v 0.1.19; Li et al. 2009). Regions of the genome annotated as repeats by RepeatMasker (<http://www.repeatmasker.org/>; last accessed May 25, 2018) or mitochondrial DNA transposed to the nuclear genome (numts) identified by blast hits to the mitochondrial sequence (at an *E*-value threshold of  $10^{-3}$ ) were removed from further analysis. We identified variable sites

across the genome using the “mpileup” command in samtools.

### Identification of Sex Chromosome Markers and Sexing of Individuals

We searched for the previously identified Y chromosome marker from the SRY gene (Palsbøll et al. 1992) in sequencing reads to identify/validate the sex of each individual. The inferred sex always matched the previously recorded sex in the field. The scaffolds of the genome assembly from a female *T. truncatus* individual were grouped into autosomal and X chromosome scaffolds based on the ratio of sequencing coverage between female and male individuals, using a previously described approach (Bidon et al. 2015). Briefly, the mean coverage of all scaffolds longer than 200 kb was calculated using BEDTools (Quinlan and Hall 2010). Scaffolds that consistently showed a female/male coverage ratio near two were deemed to be from the X chromosome. As a negative control, we also examined the coverage ratio of male/male and female/female individuals.

### Demographic History and Population Structure

Reads mapped to autosomal scaffolds longer than 100 kb were analyzed using the program PSMC (Li and Durbin 2011) to investigate temporal trends of  $N_e$  under the assumption of a generation time of 21 years and a mutation rate of  $1.21 \times 10^{-9}$  per site per year (i.e.,  $2.5 \times 10^{-8}$  per site per generation) for both dolphin species (Taylor et al. 2007; Yim et al. 2014). It is recognized that using  $\sim 75\%$  of the genome or more in the PSMC analysis results in reliable results (Nadachowska-Brzyska et al. 2016). Our PSMC analysis used 74% of the assembled genome after all the filtering. That is, regions of the genome annotated as repeats by RepeatMasker or mitochondrial DNA transposed to the nuclear genome (numts) identified by blast hits to the mitochondrial sequence (at an *E*-value threshold of  $10^{-3}$ ) were removed from PSMC analysis. Only autosomal scaffolds longer than 100 kb were used for the analyses. Another common source of error in the PSMC analysis is the use of low-coverage genome sequences. By down-sampling a high-coverage genome sequence to various levels of coverage, Nadachowska-Brzyska et al. (2016) showed that results start to differ from the original result when the coverage is below  $20\times$ . In our study, we generated whole genome sequencing data from four individuals of *T. aduncus*, with  $22$ – $180\times$  coverages ([supplementary table S1, Supplementary Material](#) online), and all four individuals show similar  $N_e$  plots from the PSMC analysis. We used publicly available data sets from six *T. truncatus* individuals in this study, including four from Northwest Pacific and two from Northwest Atlantic. Among the four Northwest Pacific samples, one has a  $43\times$  coverage and was previously analyzed using PSMC (Yim et al. 2014). Our reanalysis of this sample using PSMC yielded similar results. Three additional Northwest Pacific samples have  $10$ – $12\times$  coverages and may not be ideal for the PSMC analysis. Nonetheless, we found the  $N_e$  plots from these three individuals highly similar to that of the  $43\times$  coverage individual. Hence, the relatively low coverage does not seem to affect the PSMC analysis in the

present case. Of the two Northwest Atlantic samples, one has  $< 1\times$  coverage and is excluded from PSMC, MSMC, and SMC++ analysis. The other Northwest Atlantic sample has  $34\times$  coverage, but interestingly its  $N_e$  plot is similar to that of *T. aduncus* instead of Northwest Pacific *T. truncatus*. This observation is likely genuine rather than artifactual, because even a variation in coverage from  $10\times$  to  $43\times$  among Northwest Pacific *T. truncatus* samples does not affect the  $N_e$  trend. We found that using the *T. aduncus* or *T. truncatus* genomes as the reference for mapping reads and performing the PSMC analysis did not show any difference. To ensure comparability of the results, the *T. truncatus* genome was used as the reference for read mapping in PSMC analysis of both species.

We parameterized the initial PSMC runs with 64 atomic time intervals and 28 free intervals with the  $-p$  parameter set to “ $4 + 25 \times 2 + 4 + 6$ .” This parameter set was previously used for PSMC analysis of cetaceans (Moura et al. 2014). With these parameters, at least ten recombination events were inferred to occur in each of the time intervals within 20 iterations. However, these settings did not have sufficient resolution during the estimated split time of the species. Hence, we sought to optimize the  $-p$  and  $-t$  parameters that would provide a higher resolution of the data points. To choose an appropriate set of parameters allowing for increased resolutions, we tried a range of different values for  $-p$  (number of free atomic time intervals) and  $-t$  (upper limit of time to most recent common ancestor) parameters. For each set of parameters, we checked whether at least ten recombination events (fifth column of the PSMC output file) were inferred to occur in each of the time intervals within 20 iterations. Only those parameter combinations that satisfied these criteria were considered to avoid over-fitting. We noticed that, for higher values of the  $-t$  parameter, too few recombination events were inferred for the same values of the  $-p$  parameter. Hence, we used the PSMC default value of 5 for the parameter  $-t$  in our analysis. Increasing the  $-t$  parameter did not lead to any noticeable  $N_e$  increase in the PSMC plot into the very distant past. We used fewer time intervals and found that the parameter setting “ $20 + 13 \times 2 + 4 + 6$ ” was able to provide good resolution and still showed at least ten recombination events in each of the time intervals within 20 iterations.

To evaluate the robustness of the results to different parameters of mutation rate and generation time, we scaled the PSMC results for both species at generation times of 14, 21, and 28 years and mutation rates of  $1.0 \times 10^{-8}$ ,  $1.5 \times 10^{-8}$ ,  $2.5 \times 10^{-8}$ , and  $5 \times 10^{-8}$  per site per year. The range of generation time was chosen based on realistic values across cetacean species (Taylor et al. 2007). Furthermore, we used 100 randomizations for each of the individuals in PSMC to obtain confidence intervals of  $N_e$ . Segments used for the 100 bootstraps were of 100 kb each. The contrasting patterns in  $N_e$  trends between the two species hold for a wide range of parameters. The parameters required to generate similar  $N_e$  trends in the two species would be highly unrealistic.

To examine the potential role of population structure in generating the observed temporal trends in  $N_e$ , we performed

the pseudo-diploid analysis (Li and Durbin 2011; Prado-Martinez et al. 2013). Haploid sequences were generated from each individual using the seqtk program provided by Heng Li (<https://github.com/lh3/seqtk>; last accessed May 25, 2018). Sites with low quality were excluded using the flag  $-q$  20, and one of the alleles was randomly chosen at heterozygous sites using the flag  $-r$ . The haploid genomes from two individuals were merged to create pseudo-diploid genomes, which were then subjected to the PSMC analysis.

Although the PSMC analysis is able to infer the temporal trends of  $N_e$  based on the whole genome sequence of a single individual, the MSMC (Multiple Sequentially Markovian Coalescent) method is able to integrate information from multiple individuals of the same species to make more robust inferences (Schiffels and Durbin 2014). We used the script bamCaller.py provided along with the MSMC program to separately identify SNPs from each dolphin species. Statistical phasing of the SNP calls by the program shapeit requires at least ten individuals from each population when a SNP reference panel is unavailable. However, we do not have a reference panel. Although a previous study (Zhou et al. 2017) phased SNP data with only four individuals, they had access to a recombination rate map, which is not available for the dolphins. Hence, we converted our data to MSMC input format without phasing, using the script generate\_multihet-sep.py. The MSMC program was run with the option of “fixedRecombination” for each species separately. We did not study population divergences using the relative gene flow analysis because using unphased data can bias this analysis (Schiffels and Durbin 2014).

The MSMC method is better suited for data in which the phases of the genotype calls are known. However, in our case, accurate phasing is not possible due to the lack of a large number of samples. In such cases, the SMC++ method is an excellent alternative to the MSMC analysis. In addition to the genomic distribution of variable sites, SMC++ also utilizes information from the site frequency spectrum across individuals and has been shown to perform more reliably than MSMC, especially when using unphased data (Terhorst et al. 2017). In addition to not requiring phased data, SMC++ is also able to infer split times in diverged populations. The VCF (Variant Call Format) file with genotype information for all sites, including nonvariant sites, was generated using samtools. This file was converted to SMC format using the vcf2smc option in SMC++ program for all individuals of each population separately. The repeat annotation and numt regions identified in the genome were passed as the mask file to vcf2smc command with the  $-m$  flag. Population size histories were estimated using the estimate option in SMC++ with a mutation rate of  $1.21 \times 10^{-9}$  per site per year for both dolphin species (Taylor et al. 2007; Yim et al. 2014). Because the ancestral state could not be reliably reconstructed for our focal species, we used only the folded frequency spectrum option while running SMC++. Documentation for SMC++ suggests various parameters that need to be experimented with to identify the settings best suited for each data set. With the default settings, our data set was not generating results for more recent times.

Hence, we set the option  $-t1$  to ten generations to extend the results to recent times. However, this resulted in overfitting of the curves as well as too much oscillation. To correct this issue, we decreased the regularization penalty to a value of 5 based on recommendations in the SMC++ documentation. The parameter for thinning was set at 3,000 and “ftol” was increased to 0.01. With these settings, we were able to extend the estimates of population size by SMC++ to recent times.

We next inferred the split times for the species pair using the split option of SMC++ after estimating the joint frequency spectrum for both species with the same parameter settings as described in the previous paragraph. The split option of SMC++ provides an independent validation of the results from the pseudo-diploid analysis from PSMC. The latest version of SMC++ (version 1.11.1) does not work with data from single individuals because the site frequency estimates from single individuals are unreliable. Hence, we grouped two randomly selected individuals of *T. truncatus* (from Northwest Pacific) into population 1 and two other individuals of *T. truncatus* (from Northwest Pacific) into population 2. These two populations were used to infer the split times between *T. truncatus* individuals. Similarly, *T. aduncus* individuals were randomly grouped into two populations and used to estimate the split times among *T. aduncus* individuals.

The population structure of all sampled individuals was investigated using Principal Component Analysis (PCA) with the software ngsTools (Fumagalli et al. 2014). First, the posterior probability of genotypes was calculated using ANGSD (Korneliussen et al. 2014). These posterior probability values were then used to estimate the covariance matrix between individuals using the program ngsCovar. Finally, this covariance matrix was decomposed into eigenvectors using R to obtain principal components. Pairs of principal components were compared to identify patterns of clustering of individuals.

### Population Genetic Statistics

Single nucleotide variants at biallelic sites that had no missing data in any of the individuals were used to estimate population genetic statistics such as  $F_{st}$  (differentiation),  $d_{xy}$  (divergence), and  $\pi$  (nucleotide diversity) using Heirfstat (Goudet 2005). We further used ANGSD (Korneliussen et al. 2014) and ngsTools (Fumagalli et al. 2014) to estimate population genetic summary statistics. The values estimated from the two methods were in agreement.

### Supplementary Material

Supplementary data are available at *Molecular Biology and Evolution* online.

### Acknowledgments

We thank researchers who provided public access to sequencing data through the Short Read Archive, Yun Song and Jonathon Terhorst for advice on SMC++ analysis, and Andy Foote for valuable comments on an early draft. Byung-Yeob Kim provided some *T. aduncus* tissue samples. This

research was supported by a grant from the Collaborative Genome Program (20140428) of the Korea Institute of Marine Science and Technology Promotion (KIMST) funded by the Ministry of Oceans and Fisheries, Korea and a National Research Foundation of Korea (NRF) grant from the Korean government (MSIP) (NRF-2015R1A4A1041997) to J.K.P. J.Z. is supported by U.S. National Institutes of Health research grant R01GM120093.

### References

- Albaina N, Olsen JL, Couceiro L, Ruiz JM, Barreiro R. 2012. Recent history of the European *Nassarius nitidus* (Gastropoda): phylogeographic evidence of glacial refugia and colonization pathways. *Mar Biol.* 159(9): 1871–1884.
- Bidon T, Schreck N, Hailer F, Nilsson MA, Janke A. 2015. Genome-wide search identifies 1.9 Mb from the polar bear Y chromosome for evolutionary analyses. *Genome Biol Evol.* 7(7): 2010–2022.
- Bolger AM, Lohse M, Usadel B. 2014. Trimmomatic: a flexible trimmer for Illumina sequence data. *Bioinformatics* 30(15): 2114–2120.
- Foote A, Morin P. 2016. Genome-wide SNP data suggest complex ancestry of sympatric North Pacific killer whale ecotypes. *Heredity* 117(5): 316–310.
- Forney KA, Wade P. 2006. Worldwide distribution and abundance of killer whales. In: Estes DA, Brownell RL Jr, DeMaster DP, Doak DF, Williams TM (eds) *Whales, whaling and ocean ecosystems*. Berkeley, CA: University of California Press, pp. 145–162.
- Fumagalli M, Vieira FG, Linderot T, Nielsen R. 2014. NgsTools: methods for population genetics analyses from next-generation sequencing data. *Bioinformatics* 30(10): 1486–1487.
- Gnerre S, Maccallum I, Przybylski D, Ribeiro FJ, Burton JN, Walker BJ, Sharpe T, Hall G, Shea TP, Sykes S, et al. 2011. High-quality draft assemblies of mammalian genomes from massively parallel sequence data. *Proc Natl Acad Sci U S A.* 108(4): 1513–1518.
- Goudet J. 2005. hierfstat, a package for R to compute and test hierarchical F-statistics. *Mol Ecol Notes* 5(1): 184–186.
- Gray HWI, Nishida S, Welch AJ, Moura AE, Tanabe S, Kiani MS, Culloch R, Möller L, Natoli A, Ponnampalam LS, et al. 2018. Cryptic lineage differentiation among Indo-Pacific bottlenose dolphins (*Tursiops aduncus*) in the northwest Indian Ocean. *Mol Phylogenet Evol* 122:1–14.
- Hale PT, Barreto AS, Ross GJB. 2000. Comparative morphology and distribution of the *aduncus* and *truncatus* forms of bottlenose dolphin *Tursiops* in the Indian and Western Pacific Oceans. *Aquat Mamm.* 26:101–110.
- Hara Y, Tatsumi K, Yoshida M, Kajikawa E, Kiyonari H, Kuraku S. 2015. Optimizing and benchmarking de novo transcriptome sequencing: from library preparation to assembly evaluation. *BMC Genomics* 16:977.
- He L, Zhang A, Weese D, Li S, Li J, Zhang J. 2015. Demographic response of cutlassfish (*Trichiurus japonicus* and *T. nanhaiensis*) to fluctuating palaeo-climate and regional oceanographic conditions in the China seas. *Sci Rep.* 4(1): 6380.
- Hoegh-Guldberg O, Bruno JF. 2010. The impact of climate change on the world's marine ecosystems. *Science* 328(5985): 1523–1528.
- Kishida T. 2017. Population history of Antarctic and common minke whales inferred from individual whole-genome sequences. *Mar Mammal Sci.* 33(2): 645–652.
- Korneliussen TS, Albrechtsen A, Nielsen R. 2014. ANGSD: analysis of next generation sequencing data. *BMC Bioinformatics* 15:356.
- Learmonth JA, MacLeod CD, Santos MB, Pierce GJ, Crick HQP, Robinson RA. 2006. Potential effects of climate change on marine mammals. *Oceanogr Mar Biol.* 44:431–464.
- Leduc RG, Perrin WF, Dizon AE. 1999. Phylogenetic relationships among the Delphinid cetaceans based on full cytochrome B sequences. *Mar Mammal Sci.* 15(3): 619–648.

- Li H. 2013. Aligning sequence reads, clone sequences and assembly contigs with BWA-MEM. arXiv: 1303.3997.
- Li H, Durbin R. 2011. Inference of human population history from individual whole-genome sequences. *Nature* 475(7357): 493–496.
- Li H, Handsaker B, Wysoker A, Fennell T, Ruan J, Homer N, Marth G, Abecasis G, Durbin R. 2009. The sequence alignment/Map format and SAMtools. *Bioinformatics* 25(16): 2078–2079.
- Louis M, Viricel A, Lucas T, Peltier H, Alfonsi E, Berrow S, Brownlow A, Covelto P, Dabin W, Deaville R, et al. 2014. Habitat-driven population structure of bottlenose dolphins, *Tursiops truncatus*, in the North-East Atlantic. *Mol Ecol*. 23(4): 857–874.
- Luo R, Liu B, Xie Y, Li Z, Huang W, Yuan J, He G, Chen Y, Pan Q, Liu YY, et al. 2012. SOAPdenovo2: an empirically improved memory-efficient short-read de novo assembler. *Gigascience* 1(1): 18.
- Martien KK, Baird RW, Hedrick NM, Gorgone AM, Thieleking JL, Mcsweeney DJ, Robertson KM, Webster DL. 2012. Population structure of island-associated dolphins: evidence from mitochondrial and microsatellite markers for common bottlenose dolphins (*Tursiops truncatus*) around the main Hawaiian Islands. *Mar Mammal Sci*. 28(3): E208.
- Martin M. 2011. Cutadapt removes adapter sequences from high-throughput sequencing reads. *EMBnetjournal* 17(1): 10.
- Mazet O, Rodriguez W, Grusea S, Boitard S, Chikhi L. 2016. On the importance of being structured: instantaneous coalescence rates and human evolution-lessons for ancestral population size inference? *Heredity* 116(4): 362–371.
- Moura AE, Nielsen SCA, Vilstrup JT, Victor Moreno-Mayar J, Gilbert MTP, Gray HWI, Natoli A, Möller L, Rus Hoelzel A. 2013. Recent diversification of a marine genus (*Tursiops* spp.) tracks habitat preference and environmental change. *Syst Biol*. 62(6): 865–877.
- Moura AE, Van Rensburg CJ, Pilot M, Tehrani A, Best PB, Thornton M, Plön S, De Bruyn PJN, Worley KC, Gibbs RA, et al. 2014. Killer whale nuclear genome and mtDNA reveal widespread population bottleneck during the last glacial maximum. *Mol Biol Evol*. 31(5): 1121–1131.
- Nadachowska-Brzyska K, Burri R, Smeds L, Ellegren H. 2016. PSMC analysis of effective population sizes in molecular ecology and its application to black-and-white *Ficedula flycatchers*. *Mol Ecol*. 25(5): 1058–1072.
- O'Brien SM, Gallucci VF, Hauser L. 2013. Effects of species biology on the historical demography of sharks and their implications for likely consequences of contemporary climate change. *Conserv Genet*. 14(1): 125–144.
- Palsbøll PJ, Vader A, Bakke I, El-Gewely MR. 1992. Determination of gender in cetaceans by the polymerase chain reaction. *Can J Zool*. 70(11): 2166–2170.
- Parra G, Bradnam K, Korf I. 2007. CEGMA: a pipeline to accurately annotate core genes in eukaryotic genomes. *Bioinformatics* 23(9): 1061–1067.
- Prado-Martinez J, Sudmant PH, Kidd JM, Li H, Kelley JL, Lorente-Galdos B, Veeramah KR, Woerner AE, O'Connor TD, Santpere G, et al. 2013. Great ape genetic diversity and population history. *Nature* 499(7459): 471–475.
- Quinlan AR, Hall IM. 2010. BEDTools: a flexible suite of utilities for comparing genomic features. *Bioinformatics* 26(6): 841–842.
- Schiffels S, Durbin R. 2014. Inferring human population size and separation history from multiple genome sequences. *Nat Genet*. 46(8): 919–925.
- Simão FA, Waterhouse RM, Ioannidis P, Kriventseva EV, Zdobnov EM. 2015. BUSCO: assessing genome assembly and annotation completeness with single-copy orthologs. *Bioinformatics* 31:3210–3212.
- Song S, Sliwerska E, Emery S, Kidd JM. 2017. Modeling human population separation history using physically phased genomes. *Genetics* 205(1): 385–395.
- Song S, Sliwerska E, Kidd JM. 2014. Population split time estimation and X to autosome effective population size differences inferred using physically phased genomes. *BioRxiv*. doi: <https://doi.org/10.1101/008367>.
- Tatusova T, Ciufu S, Fedorov B, O'Neill K, Tolstoy I. 2014. RefSeq microbial genomes database: new representation and annotation strategy. *Nucleic Acids Res*. 42(D1): D553–D559.
- Taylor BL, Chivers SJ, Larese J, Perrin WF. 2007. Generation length and percent mature estimates for IUCN assessments of cetaceans. Administrative report LJ-07-01. NOAA, La Jolla, USA; 2007. 24 pp.
- Terhorst J, Kamm JA, Song YS. 2017. Robust and scalable inference of population history from hundreds of unphased whole genomes. *Nat Genet*. 49(2): 303–309.
- Thuiller W. 2007. Biodiversity: climate change and the ecologist. *Nature* 448(7153): 550–552.
- Vilstrup JT, Ho SY, Foote AD, Morin PA, Krebs D, Krützen M, Parra GJ, Robertson KM, De Stephanis R, Verborgh P, et al. 2011. Mitogenomic phylogenetic analyses of the Delphinidae with an emphasis on the Globicephalinae. *BMC Evol Biol*. 11:65.
- Wang JY, Chou LS, White BN. 1999. Mitochondrial DNA analysis of sympatric morphotypes of bottlenose dolphins (genus: *Tursiops*) in Chinese waters. *Mol Ecol*. 8(10): 1603–1612.
- Wang JY, Chou LS, White BN. 2000. Differences in the external morphology of two sympatric species of bottlenose dolphins (genus *Tursiops*) in the waters of China. *J Mammal*. 81(4): 1157–1165.
- Wang JY, Chou LS, White BN. 2000. Osteological differences between two sympatric forms of bottlenose dolphins (genus *Tursiops*) in Chinese waters. *J Zool*. 252(2): 147–162.
- Yim HS, Cho YS, Guang X, Kang SG, Jeong JY, Cha SS, Oh HM, Lee JH, Yang EC, Kwon KK, et al. 2014. Minke whale genome and aquatic adaptation in cetaceans. *Nat Genet*. 46:88–92.
- Zhou Y, Massonnet M, Sanjak JS, Cantu D, Gaut BS. 2017. Evolutionary genomics of grape (*Vitis vinifera* ssp. *vinifera*) domestication. *Proc Natl Acad Sci U S A*. 144:11715–11720.